Mol Neurobiol (2018) 55:2403–2419
DOI 10.1007/s12035-017-0496-4

Neuroprotective Effects of Temsirolimus in Animal Models of Parkinson's Disease

Rosalba Siracusa[1] · **Irene Paterniti**[1] · **Marika Cordaro**[1] · **Rosalia Crupi**[1] · **Giuseppe Bruschetta**[1] · **Michela Campolo**[1] · **Salvatore Cuzzocrea**[1,2] · **Emanuela Esposito**[1]

Received: 13 February 2017 / Accepted: 14 March 2017 / Published online: 29 March 2017

Abstract Parkinson's disease (PD) is a disorder caused by degeneration of dopaminergic neurons. At the moment, there is no cure. Recent studies have shown that autophagy may have a protective function against the advance of a number of neurodegenerative diseases. Temsirolimus is an analogue of rapamycin that induces autophagy by inhibiting mammalian target of rapamycin complex 1. For this purpose, in the present study we investigated the neuroprotective effects of temsirolimus (5 mg/kg intraperitoneal) on 1-methyl-4-phenyl-1,2,3,6-tetrahydropyridine-induced (MPTP) neurotoxicity in in vivo model of PD. At the end of the experiment, brain tissues were processed for histological, immunohistochemical, Western blot, and immunofluorescent analysis. Treatment with temsirolimus significantly ameliorated behavioral deficits, increased the expression of specific markers of PD such as tyrosine hydroxylase, dopamine transporter, as well as decreased the upregulation of α-synuclein in the substantia nigra after MPTP induction. Furthermore, Western blot and immunohistochemistry analysis showed that temsirolimus administration significantly increased autophagy process. In fact, treatment with temsirolimus maintained high Beclin-1, p62, and microtubule-associated protein 1A/1B-light chain 3 expression and inhibited the p70S6K expression. In addition, we showed that temsirolimus has also anti-inflammatory properties as assessed by the significant inhibition of the expression of mitogen-activated protein kinases such as p-JNK, p-p38, and p-ERK, and the restored levels of neurotrophic factor expression such as BDNF and NT-3. On the basis of this evidence, we clearly demonstrate that temsirolimus is able to modulate both the autophagic process and the neuroinflammatory pathway involved in PD, actions which may underlie its neuroprotective effect.

Keywords Neurodegenerative disease · Autophagy · Neuroinflammation · Neuroprotection · Rapamycin

Introduction

Parkinson's diseases is one of the most widespread degenerative neurological disorder that affects people over 60, characterized by the progressive loss of dopaminergic neurons both in the central and in the peripheral nervous system [1, 2]. The damage in these cells determinate a reduced release of dopamine that functions as a neurotransmitter that regulates movement and coordination. Moreover, Parkinson's disease (PD) is characterized by the presence of Lewy bodies (LB) that are eosinophilic cytoplasmatic inclusions composed by insoluble aggregates of different proteins, mainly α-synuclein and ubiquitin [3, 4]. Current therapeutic approach is based to ameliorate principally clinical manifestations of the disorder such as resting tremor, rigidity, and hypokinesia; nevertheless, there is no effective cure that can reduce the underlying neuron degeneration and loss. Although the mechanism underlying disease initiation and progression is still unknown, recently a lot of studies focused the attention on neuroinflammation that is another important feature in PD [5–7]. α-Synuclein released from neuronal cells could also be transferred to and accumulate in astrocytes inducing expression of genes that are associated with strong inflammatory response; in particular, increased expression of pro-inflammatory cytokines and

✉ Emanuela Esposito
eesposito@unime.it

[1] Department of Chemical, Biological, Pharmaceutical and Environmental Science, University of Messina, Viale Ferdinando Stagno D'Alcontres n, 31 98166 Messina, Italy

[2] Department of Pharmacological and Physiological Science, Saint Louis University School of Medicine, Saint Louis, MO, USA

chemokines has detected in the brain parenchyma and CSF of human PD patients suggesting that α-synuclein mediates neuroinflammation [8]. Moreover, recent studies are based on the role of proteasomal, lysosomal, and autophagic pathways involved in α-synuclein clearance in PD [9, 10]. It has been shown that autophagic pathway helps in cell survival by removing unwanted cellular organelle and protein aggregates [11]. Autophagy is a multi-step process, comprising the formation of double membrane structures noted as autophagosomes that fuse with lysosomes in order to form autophagolysosomes, whose contents, such as misfolded proteins and cellular metabolic discards, are then degraded [12]. There are recent evidence to suggest that change in costitutive autophagy in neurons can impact the number and quality of synaptic plasticity and regulation of presynaptic signaling. Many neurodevelopmental disorders are associated with dysfunction in autophagy-related pathways (e.g., mTOR) [13]. Recent studies reveal that autophagy is constitutively active in healthy neurons and can be considered as a beneficial response of neurons in repairing or remodeling damaged cellular components necessary for sustaining normal neuronal function and survival [14, 15]. In particular in PD, autophagy has been found as a predominant pathway involved in α-synuclein clearance, supporting this possibility is the finding that α-synuclein is detected inside vesicles with autophagic morphology and the autophagy activator, such as rapamycin, stimulates its clearance [16–18]. Rapamycin is a pharmacological compound that is capable to provide neuroprotection in numerous experimental models of neurodegenerative diseases, including AD, PD, Huntington's disease, and spinocerebellar ataxia type 3 [19]. Rapamycin is a macrolide that particularly inhibits mammalian target of rapamycin (mTOR) that is a serine/threonine protein kinase, member of the phosphatidylinositol 3-kinase-related kinase protein family, that regulates cell growth, cell proliferation, cell survival, protein synthesis, and inhibition of autophagy [20–22]. Rapamycin inhibits the mTORC1 pathways thus enhancing autophagy. Although the beneficial effects of rapamycin, this compound may causes unwanted side effects such as peripheral edema, hypertriglyceridemia, hypertension, hypercholesterolemia, increasing of creatinina, constipation, abdominal pain, diarrhea, headache, fever, urinary tract infection, anemia, nausea, arthralgia, pain, and thrombocytopenia [23–26]. Thus, recent findings suggested that a newly developed analogue of rapamycin, temsirolimus, could possess the same beneficial effects of rapamycin with lower side effects [27, 28]. It has been demonstrated that temsirolimus possesses neuroprotective effects in animal models of HD and spinocerebellar ataxia type 3, two neurodegenerative diseases caused by accumulation of aberrant proteins inside the brain [29, 30]. Temsirolimus actually is approved by the U.S. Food and Drug Administration and the European Medicines Agency for the treatment of renal cell carcinoma [31]. In this framework, stimulation of autophagy represents promising new strategies to prevent or decrease the progression of PD; thus based on the above evidence, we carried out the present study to investigate, in an animal model of PD, the potential neuroprotective effects of temsirolimus linked to induction of autophagy and modulation of neuroinflammation.

Material and Methods

Animals

C57/BL6 mice (male 25–30 g; Harlan Nossan, Milan, Italy) were accommodated in a controlled environment and equipped with standard rodent chow and water. Mice were housed in steel cages in a room kept at 22 ± 1 °C with a 12-h light, 12-h dark cycle. Mice were acclimatized to their habitat for 1 week and they had ad libitum access to tap water and rodent standard diet. The University of Messina Review Board for the care of animals approved the study. All animal experiments complied with regulations in Italy (D.M. 116,192) as well as the EU regulations (O.J. of E.C. L 358/1 12/18/1986).

MPTP-Induced PD and Treatments

Eight-week-old male C57/BL6 mice were treated with MPTP or saline. For MPTP intoxication, mice received four i.p. injections of MPTP (20 mg/kg; Sigma, Milan Italy) in saline solution at 2 h intervals in 1 day: total dose per mouse was 80 mg/kg. For temsirolimus treatment (5 mg/kg in 10% dimethyl sulfoxide), mice received i.p. temsirolimus starting 24 h after the first MPTP administration and continuing through 7 additional days after the last administration of MPTP. Sham animals received vehicle only. Eight days after MPTP injection, mice were sacrificed by decapitation. Brains were dissected out, and midbrains were isolated and processed. The dose of MPTP (20 mg/kg) and temsirolimus (5 mg/kg) used was based on previous in vivo studies [32–34].

Experimental Groups

The animals were arbitrarily allocated into the following groups:

Group 1. Sham+Veh = Vehicle solution (saline) was administered i.p. during the 1st day, like MPTP protocol. ($N = 10$)

Group 2. Sham+temsirolimus = Same as the Sham + Veh group, but temsirolimus (5 mg/kg body weight, soluble 10% dimethyl sulfoxide, i.p.) was administered starting 24 h after the first vehicle solution

injection and continuing through 7 additional days after the last administration of saline. ($N = 10$)

Group 3. MPTP+Veh = MPTP solution was administered as described for administration of saline. ($N = 10$)

Group 4. MPTP+temsirolimus = Same as the MPTP + Veh group, but temsirolimus (at a dose of 5 mg/kg body weight, soluble 10% dimethyl sulfoxide, i.p.) was administered starting 24 h after the first MPTP administration and continuing through 7 additional days after the last injection of MPTP. ($N = 10$)

Preparation of Cytosolic and Nuclear Extracts from Brain and Western Blot Analysis

To perform Western blot analysis, the mice were anesthetized by xylazine and ketamine (0.16 and 2.6 mg/kg body weight, respectively, given i.p.) and after decapitated with large bandage scissors. Brains of each mouse were quickly removed and suspended in extraction buffer A comprising 20 mM leupeptin, 0.15 mM pepstatin A, 0.2 mM PMSF, 1 mM sodium orthovanadate, homogenized at the maximum setting for 2 min, and centrifuged at 12,000 rpm for 4 min at 4 °C. Supernatants represented the cytosolic fraction. The pellets, which contains enriched nuclei, were resuspended in buffer B containing 10 mM Tris–HCl pH 7.4, 150 mM NaCl, 1 mM EGTA, 1% Triton X-100, 1 mM EDTA, 0.2 mM PMSF, 20 mm leupeptin, and 0.2 mM sodium orthovanadate. After centrifugation for 10 min at 12,000 rpm at 4 °C, the supernatants containing the nuclear protein were stored at −80 °C for further analysis. Protein concentrations were assessed by the Bio-Rad protein assay using bovine serum albumin as standard. Briefly, samples were heated to 100 °C for 5 min, and equal amounts of protein were separated on 12% SDS-PAGE gel and transferred to nitrocellulose membrane. The expression of α-synuclein, p62, p70S6K, Beclin1, MAP-LC3, p-JNK, p-p38, p-ERK, GFAP, and Iba-1 was quantified in cytosolic fractions. Specific primary antibody, rabbit polyclonal anti-α-synuclein (1:500; Santa Cruz Biotechnology), rabbit polyclonal anti-p62 (1:1000; Cell Signaling), rabbit polyclonal anti-p70S6K (1:1000; Cell Signaling), rabbit polyclonal anti-Beclin1 (1:1000; Cell Signaling), rabbit polyclonal anti-MAP-LC3 (1:500; Santa Cruz Biotechnology), mouse monoclonal anti-p-JNK (1:500; Santa Cruz Biotechnology), mouse monoclonal anti-p-p38 (1:1000; Cell Signaling), mouse monoclonal anti-p-ERK (1:500; Santa Cruz Biotechnology), mouse monoclonal anti-GFAP (Santa Cruz Biotechnology; 1:1000), and mouse monoclonal anti-Iba-1 (Santa Cruz Biotechnology; 1:1000) were mixed in 1× phosphate-buffered saline (PBS), 5% *w/v* nonfat dried milk, and 0.1% Tween-20 and incubated at 4 °C overnight. Membranes were then incubated with peroxidase-conjugated bovine anti-mouse IgG secondary antibody or peroxidase-conjugated goat anti-rabbit IgG (1:2000, Jackson ImmunoResearch) for 1 h at room temperature. To make sure that blots were loaded with equal amounts of proteic lysates, they were also incubated with the antibody agonist mouse monoclonal β-actin (1:5000; Santa Cruz Biotechnology) and mouse monoclonal anti-JNK (1:1000; Santa Cruz Biotechnology), mouse monoclonal anti-p38 (1:1000; Cell Signaling), and mouse monoclonal anti-ERK (1:500; Santa Cruz Biotechnology). Signals were detected with enhanced chemiluminescence detection system reagent according to the manufacturer's instructions (SuperSignal West Pico Chemiluminescent Substrate, Pierce). Relative expression of protein bands was quantified by densitometry with BIORAD ChemiDoc™XRS+software and standardized to β-actin levels. Images of blot signals (8 bit/600 dpi resolution) were transferred to analysis software (Image Quant TL, v2003).

Immunohistochemical Localization of TH, DAT, and α-Synuclein

At the end of the experiment, the mice were anesthetized by xylazine and ketamine (0.16 and 2.6 mg/kg body weight, respectively, given i.p.) and after decapitated with large bandage scissors. Brains of each mouse were removed and were fixed in 10% (*w/v*) PBS-buffered formalin for 24 h and 7 μm sections were prepared from paraffin fixed tissues. After deparaffinization, endogenous peroxidase was reduced with 0.3% (*v/v*) H_2O_2 60% (*v/v*) methanol for 30 min. The sections were permeabilized with 0.1% (*v/v*) Triton X-100 in PBS for 20 min. Non-specific adsorption was minimized incubating the section in 2% (*v/v*) normal horse serum in PBS for 20 min. Endogenous biotin or avidin binding points were blocked by sequential incubation for 15 min with avidin and biotin (Vector Laboratories, Burlingame, CA). Sections were incubated overnight with anti-TH antibody (Millipore, 1:500 in PBS, *v/v*), anti-DAT antibody (Santa Cruz Biotechnology, 1:300 in PBS, *v/v*), anti-α-synuclein antibody (Santa Cruz Biotechnology, 1:50 in PBS, *v/v*), anti-Beclin-1 antibody (Santa Cruz Biotechnology, 1:250 in PBS, *v/v*), and anti-mTOR (Cell Signaling, 1:250 in PBS, *v/v*). Sections were cleaned with PBS and incubated with secondary antibody. Specific category was detected with a biotin-conjugated goat anti-rabbit IgG and avidin-biotin peroxidase complex (Vector Labs Inc., Burlingame, CA). To verify the binding specificity for different antibodies, some sections were also incubated with only primary or secondary antibody; no positive staining was observed in these sections. The sections were quantitatively evaluated for a variance in immunoreactivity by computer-assisted color image analysis (Leica QWin V3, Cambridge, UK). Immunoreactivity was quantized within five random fields at ×20 and ×40 magnifications. The fraction of positive staining as a function of total tissue area was determined [35]. In sham mice, the central areas of corresponding

tissue sections were taken as reference points and a comparable number of optical fields were calculated. All the immunocytochemistry analysis was carried out without knowledge of [36] the treatments.

Stereology

Unbiased counting of TH^+ dopaminergic neurons within the SN was performed as described previously [36]. Briefly, at the end of the experiment, mice were killed and perfused intracardially with PBS and the brains were removed and post-fixed in 4% paraformaldehyde at 4 °C overnight. Serial sections (40 μm thick) were cut from each block through the SN in the coronal plane by a vibratome. Every fourth free floating section was incubated with polyclonal rabbit anti-TH (1:400, Millipore) overnight and processed with the ABC method (Vector Laboratories, Burlingame, CA). Sections were counterstained with cresyl violet, a Nissl stain, and cover-slipped. TH^+ cells were immunoreactive for TH while TH^- cells were not immunoreactive for TH but were Nissl stained. The stereologist was blind to the treatment received.

For each mouse brain, five selected representative sections of the SNpc were analyzed with StereoInvestigator software (Microbrightfield, Williston, VT).

Immunofluorescence Staining

After deparaffinization and rehydration, detection of brain-derived neurotrophic factor (BDNF), neurotrophins 3 (NT-3), GFAP, Iba-1, TH, α-synuclein, Beclin-1, and mTOR was carried out after boiling in 0.1 M citrate buffer for 1 min. Non-specific adsorption was diminished by incubating the section in 2% (vol/vol) normal goat serum in PBS for 20 min. Sections were incubated with mouse monoclonal anti-GFAP (Santa Cruz Biotechnology; 1:200 in PBS, *v*/*v*), or with mouse monoclonal anti-Iba-1 (Santa Cruz Biotechnology; 1:200 in PBS, *v*/*v*), or with rabbit polyclonal anti-BDNF (Santa Cruz Biotechnology; 1:200 in PBS, *v*/*v*), or with rabbit polyclonal anti-NT-3 (Santa Cruz Biotechnology; 1:100 in PBS, *v*/*v*), or with mouse monoclonal anti-TH (Millipore; 1:100 in PBS, *v*/*v*), or with rabbit polyclonal anti-α-synuclein (Santa Cruz Biotechnology; 1:100 in PBS, *v*/*v*), or with rabbit polyclonal anti-Beclin-1 (Santa Cruz Biotechnology; 1:100 in PBS, *v*/*v*), or with rabbit polyclonal anti-mTOR (Cell Signaling; 1:100 in PBS, *v*/*v*) Abs in a humidified chamber O/N at 37 °C. Sections were washed with PBS and were incubated with secondary antibody TEXAS RED-conjugated anti-rabbit Alexa Fluor-594 antibody (1:1000 in PBS, *v*/*v* Molecular Probes, UK) and with FITC-conjugated anti-mouse Alexa Fluor-488 antibody (1:2000 *v*/*v* Molecular Probes, UK) for 1 h at 37 °C. Sections were laved and for nuclear staining 4′,6′-diamidino-2-phenylindole (DAPI; Hoechst, Frankfurt; Germany) 2 μg/ml in PBS was added. Sections were seen and photographed using a Leica DM2000 microscope (Leica, Milan Italy). Optical sections of fluorescence samples were obtained using an Ar laser (458 nm) and a HeNe laser (543 nm), a laser UV (361–365 nm) at a 1-min, 2-s scanning speed with up to 8 averages; 1.5-μm sections were acquired using a pinhole of 250. Contrast and illumination were established by examining the most intensely labeled pixels and applying backgrounds that allowed clear image of structural details while keeping the highest pixel intensities close to 200. The same backgrounds were used for all images acquired from the other samples that had been managed in parallel. Digital images were collected and figure montages arranged using Adobe Photoshop CS6 (Adobe Systems; Milan Italy).

Behavioral Testing

Behavioral evaluations on all mice were made 1 day prior to, and 8 days after, MPTP injection:

Motor Observation

Rotarod Test

Behavioral assessments on each mouse were made 1 day prior to, and 8 days after, MPTP injection. Motor performance was assessed with a rotary rod apparatus using a protocol similar to that described [37]. For the rotarod tests, the rotadrum was filled with water to a level just below the bottom of the rod. The mice were placed on the rotating rod and the time until they fell off was recorded. This was repeated (with a rest period that increased by 5 s with each fall) until the total time on the rod for the control group was 5 min. Both the total time spent on the rotating rod and the total number of falls for each mouse was recorded.

Catalepsy Test

Catalepsy, defined as a reduced ability to initiate movement and a failure to correct posture, was measured with the help of bar test. To test for catalepsy, mice were positioned so that their hindquarters were on the bench and their forelimbs rested on a 1-cm-diameter horizontal bar, 4 cm above the bench. The time the mice maintained this position was recorded by stopwatch to a maximum of 180 s. The catalepsy test was evaluated at 8 days after MPTP injection [38]. Mice were judged to be cataleptic if they maintained this position for 30 s or more. Animals were put back in their home cage after each measurement of catalepsy. All values are expressed as the means ± SEM.

Neuropsychological Evaluation

FST

The test is based on that described by Porsolt et al. [39]. A vertical glass cylinder (25 cm high, 14 cm in diameter) was filled with 27 °C water to a depth of 20 cm. Each mouse was gently placed in the cylinder for 6 min and the duration of floating (i.e., the time during which mice made only the small movements necessary to keep their heads above water) was scored. Immobility time was analyzed during the last 4 min period of the test.

Elevated plus-Maze Test

The elevated plus-maze protocol was used to measure contextual anxiety and performed as previously described [40, 41]. Briefly, the apparatus was comprised of two open arms and two closed arms in black Plexiglas with a light gray floor, which extended from a central platform. Mice were placed individually on open arm and allowed to explore the maze for 5 min. An arm entry was counted only when all four paws were inside the arm. The apparatus was cleaned with a solution containing 30% ethanol after each 5 min run and wiped dry before the next test.

Materials

Unless otherwise stated, all compounds were obtained from Sigma-Aldrich. All other chemicals were of the highest commercial grade available. All stock solutions were prepared in non-pyrogenic saline (0.9% NaCl, Baxter, Milan, Italy) or 10% dimethyl sulfoxide.

Statistical Evaluation

All values in the figures and the text are expressed as mean ± SEM. Results shown in the figures are representative of at least three experiments performed on different in vivo experimental days. In each experiment, we used 10 animals per group, unless otherwise indicated. The results were analyzed by one-way analysis of variance followed by a Bonferroni post-hoc test for multiple comparisons. A p value of less than 0.05 was considered significant.

Results

Temsirolimus Treatment Reduced Behavioral Impairments Induced by MPTP Intoxication

The motor function in the entire experimental group was assessed using a Rotarod apparatus. At 8 days after MPTP injection, mice showed a significant motor disorder as indicated by a reduce in time period spent on the Rotarod and by a greater number of falls, while treatment with temsirolimus significantly reduced this motor dysfunction (Fig. 1 a). Moreover, the MPTP administration produced a significant cataleptic effect in mice. In fact at 8 days after MPTP injection, mice showed an increased significant cataleptic symptoms increase. On the contrary, the daily temsirolimus (5 mg/kg i.p.) administration significantly reduced the catalepsy duration induced by MPTP (Fig. 1 b). Furthermore, at 8th days after MPTP-intoxication, mice exhibited non-motor symptoms PD-associated as clearly demonstrated by the significantly increased immobility time in the FST. The MPTP-induced immobility was significantly reversed by the temsirolimus daily treatment (Fig. 1 c). Moreover, mice were then observed for anxiety-like behavior in the elevated plus-maze (EPM). The behavioral test that we performed indicated an important increase in the percentage of time spent in the open arms and in the number of entries in the open arms after temsirolimus treatment, compared to the MPTP group (Fig. 1 d, d′).

Temsirolimus Treatment Reduced Loss of TH Expression and Plasma Membrane DAT in the SN Induced by MPTP Administration

Moreover, in order to study better the effect of temsirolimus treatment on the dopamine pathway, we also evaluated the expression of TH and DAT. In the SN at 8 days after MPTP administration, a significant loss of TH-positive cells was clearly demonstrated (Fig. 2 c, c′ and see relative densitometry analysis e), while the treatment with temsirolimus considerably reduced the loss of TH-positive neurons in the SN (Fig. 2 d, d′ and see relative densitometry analysis e).

Unbiased stereology of nigral TH-positive neurons performed 8 days after MPTP intoxication showed significant neuroprotection by temsirolimus treatment. We observed a significantly decline in the number of TH-positive neurons in mice after MPTP injection, compared to Sham and Sham+temsirolimus groups. This loss decreased following temsirolimus treatment (Fig. 2 f, g). Similarly, Nissl-stained neurons were depleted significantly by MPTP lesioning but not in animals that had been treated with temsirolimus (Fig. 2 f, h).

Furthermore, we revealed an important loss of DAT in MPTP-injected animals at the level of the midbrain (Fig. 3 c, c′ and see relative densitometry analysis e), whereas temsirolimus treatment significantly restored the levels of DAT comparable to control group (Fig. 3 d, d′ and see relative densitometry analysis e). Finally, to determine the status of the nigrostriatal pathway, we evaluated the dopaminergic terminals in the striatum, where we observed a trend similar to that shown in the midbrain. Briefly, we observed a significantly loss of DAT in mice after MPTP injection (Fig. 3 h, and see

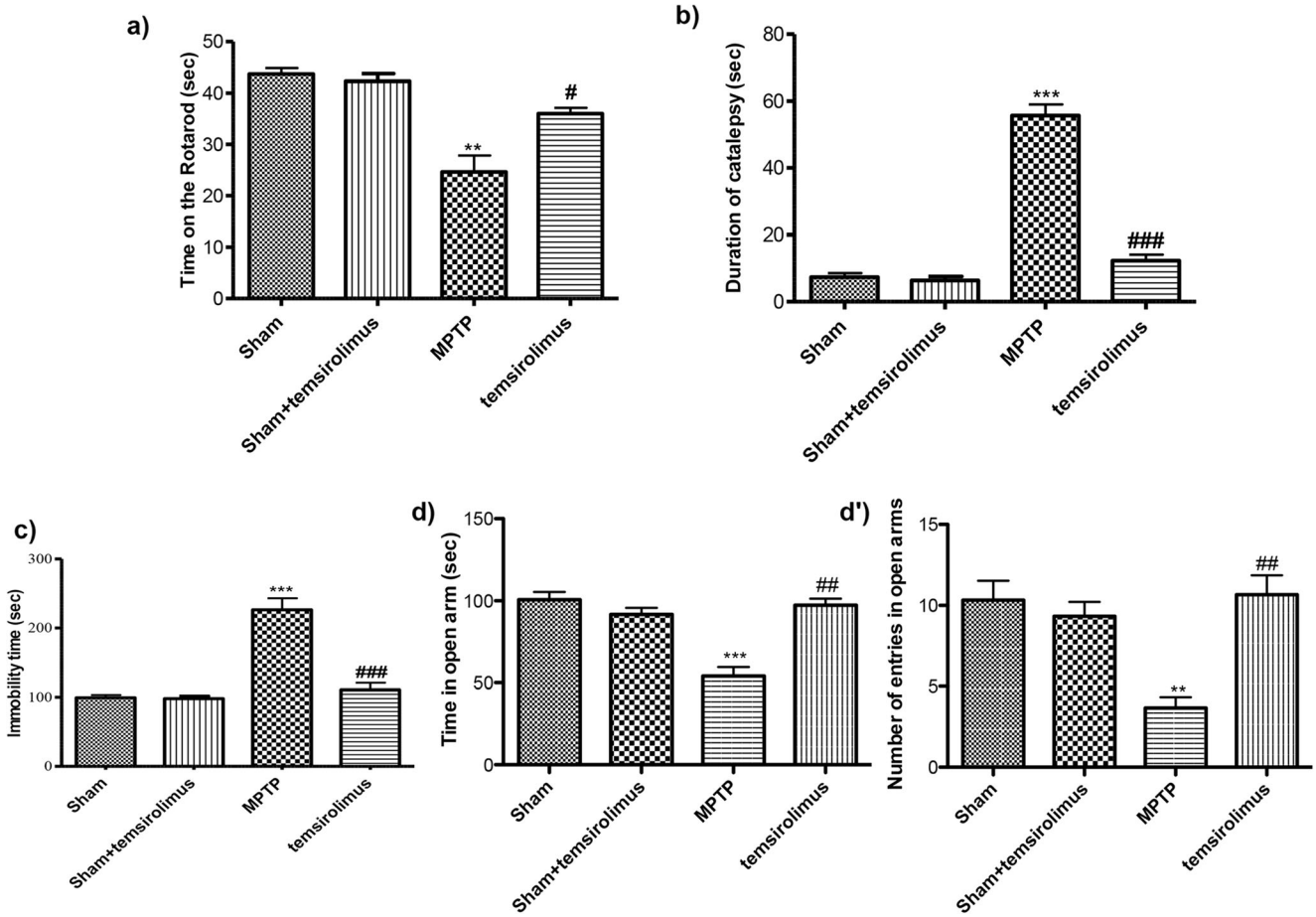

Fig. 1 Effect of temsirolimus on behavioral impairments induced by MPTP intoxication. (*a*) Motor function was assessed using a Rotarod apparatus. At 8 days, mice exhibited a significant motor dysfunction as indicated by a decrease in time spent on the Rotarod. Temsirolimus treatment blunted the motor dysfunction in mice. Values are mean ± SEM ($N = 10$ per group). $^{**}p < 0.01$ vs Sham and Sham+temsirolimus; $\#p < 0.05$ vs MPTP. (*b*) Catalepsy was evaluated according to the standard bar hanging procedure; this motor test showed that temsirolimus treatment reduced behavioral impairment induced by MPTP. $^{***}p < 0.001$ vs Sham and Sham+temsirolimus; $\#\#\#p < 0.001$ vs MPTP. (*c*) Effects of chronic temsirolimus treatment in the mouse FST 8 days after MPTP injection. Results are expressed as mean of mobility duration in seconds. $^{***}p < 0.001$ vs Sham and Sham+temsirolimus; $\#\#\#p < 0.001$ vs MPTP. (*d*, *d*′) Effect of temsirolimus treatment on anxiety behaviors in the EPM. Anxiety is expressed as mean total entries in the open arms and number of entries in open arms. (*d*) $^{***}p < 0.05$ vs Sham and Sham+temsirolimus; $\#\#p < 0.01$ vs MPTP; (*d*′) $^{**}p < 0.05$ vs Sham and Sham+temsirolimus; $\#\#p < 0.01$ vs MPTP

relative densitometry analysis l), compared to Sham and Sham+temsirolimus groups (Fig. 3 f, g and see relative densitometry analysis l), while temsirolimus treatment significantly reduced the loss of DAT (Fig. 3 i and see relative densitometry analysis l).

Temsirolimus Treatment Reduced α-Synuclein in the SN Induced by MPTP-Intoxication

α-Synuclein is the major component of intraneuronal protein aggregates designated as Lewy bodies, an important pathological characteristic of PD. For this reason, to demonstrate the capability of temsirolimus to counteract α-synuclein-induced degeneration, we evaluated in the cytosolic fraction the expression of this protein by Western blot. An important increase of α-synuclein expression was observed in the SN at 8 days after MPTP injection, while the treatment with temsirolimus significantly reduced levels of α-synuclein in the SN (Fig. 4 a, and see relative densitometry analysis a′). Also, by immunohistochemical analysis, we observed a significant immunoreactivity in MPTP-injured mice (Fig. 4 d, d′ and see densitometric analysis f) compared to control mice (Fig. 4 a, a′; b, b′). Instead, the treatment with temsirolimus decreased significantly α-synuclein expression in the SN after MPTP-intoxication (Fig. 4 e, e′ and see densitometric analysis f). Also, to evaluate the α-synuclein accumulation in the dopaminergic neurons, we assessed a double staining between TH (green) and α-synuclein (red). We observed the absence of α-synuclein into the dopaminergic neurons TH-positive in Sham group (Fig. 5 c), while after MPTP intoxication there was an increasing accumulation of α-synuclein in the TH-positive neurons (Fig. 5 f). In the group treated with temsirolimus, we noticed a significantly decreased of α-synuclein levels into the dopaminergic neurons (Fig. 5 i).

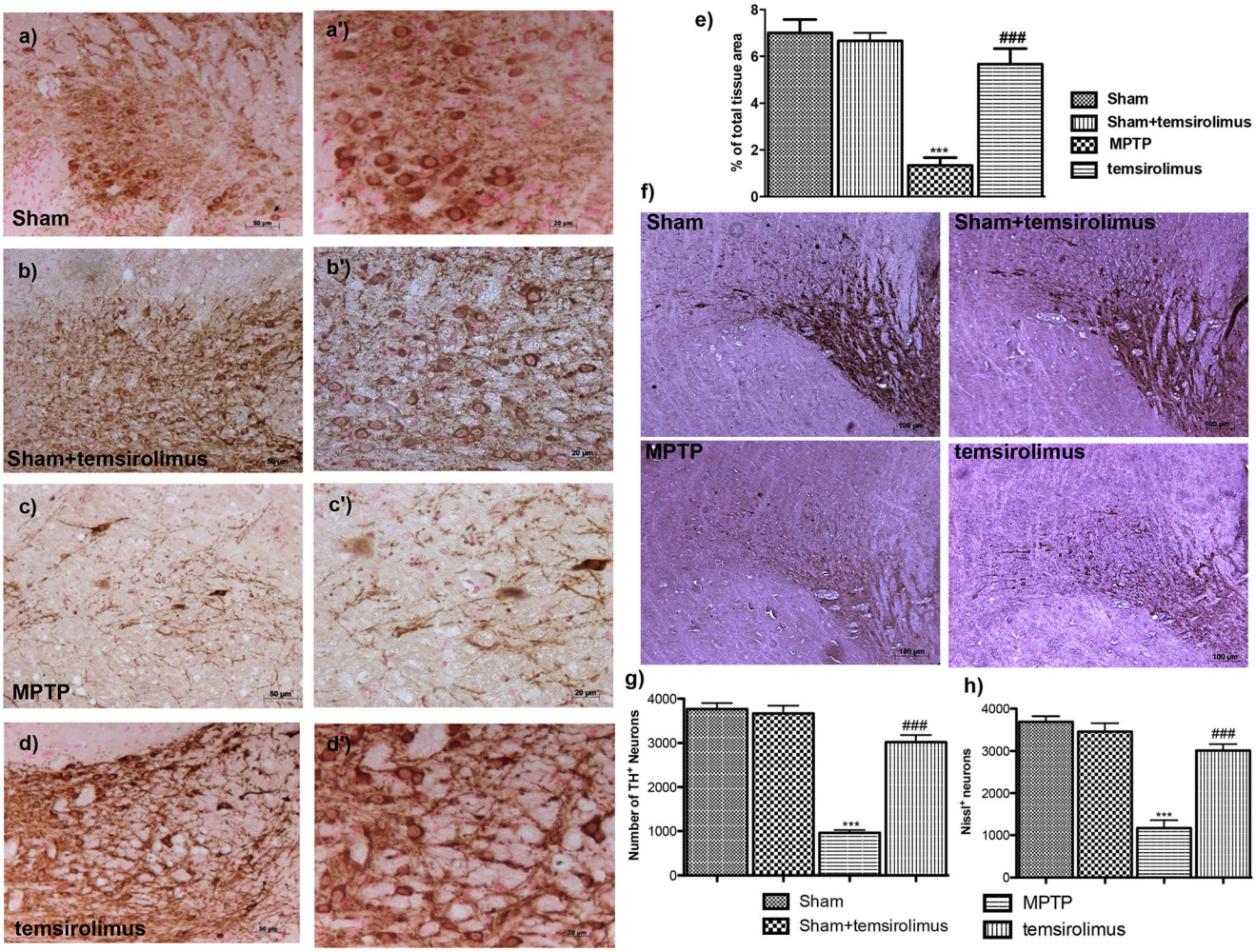

Fig. 2 Effects of temsirolimus on TH expression in SN of MPTP-treated mice. Midbrain was stained with antibodies against TH. Immunohistochemical analysis of midbrain obtained from mice after MPTP intoxication revealed a marked loss of TH-positive cells (*c*, *c′* see densitometric analysis, *e*) compared with Sham and Sham+ temsirolimus mice (*a*, *a′*; *b*, *b′* and see densitometric analysis, *e*). Mice subjected to treatment with temsirolimus revealed a positive staining for TH (*d*, *d′* see densitometric analysis, *e*). Data are expressed as a percentage of total tissue area and are means ± SE of 5 mice/group. ***$p < 0.001$ vs Sham and Sham+temsirolimus; ###$p < 0.001$ vs MPTP. Stereological counting of TH-positive and cresyl-violet positive neurons in sections of the substantia nigra from one hemisphere (*g*, *h*). Representative images of TH immunohistochemistry of midbrain sections and counterstained with cresyl violet (*f*). *Scale bar* 100 μm. Each data are expressed as a number of TH^+ and $Nissl^+$ neurons and are mean ± SEM from $N = 5$ mice/group. ***$p < 0.001$ vs Sham and Sham+temsirolimus; ###$p < 0.001$ vs MPTP (*g*, *h*)

Effect of Temsirolimus on the Stimulation of Autophagy: Expression of p70S6K, Beclin-1, p62, LC3, and mTOR

To study the effect of temsirolimus on autophagy, we examined levels of proteins implicated in the regulation and formation of autophagosomes. mTOR is a central signal integrator that functions as a checkpoint upstream of phosphatidylinositol 3-kinase (PI3K) and downstream of p70S6K. In a first time, according to these evidences, by Western blot analysis, we demonstrated in the cytosolic fraction that treatment with temsirolimus reduced p70S6K expression inhibiting mTOR and stimulating the autophagy (Fig. 6 a and see relative densitometry analysis a′). Furthermore, always in the cytosolic fraction to confirm the ability of temsilorimus to promote autophagy, the levels of specific proteins were determined. Beclin-1 interacts with various cofactors inducing autophagy. We observed a significant increase of Beclin-1 expression in temsirolimus-treated mice (Fig. 6 b, and see relative densitometry analysis b′). For more accurate quantification of temsirolimus effects on autophagy process, we examined levels of p62 in the cytosolic fraction. We detected that p62 expression increases in a no significant manner after MPTP-intoxication. Treatment with temsirolimus significantly increased p62 expression in the MPTP+temsirolimus group (Fig. 6 c and see relative densitometry analysis c′). p62 also interacts with a central component of the machine autophagy, autophagic marker LC3, and carries the altered proteins to degradation by autophagy. Therefore, we showed, in the

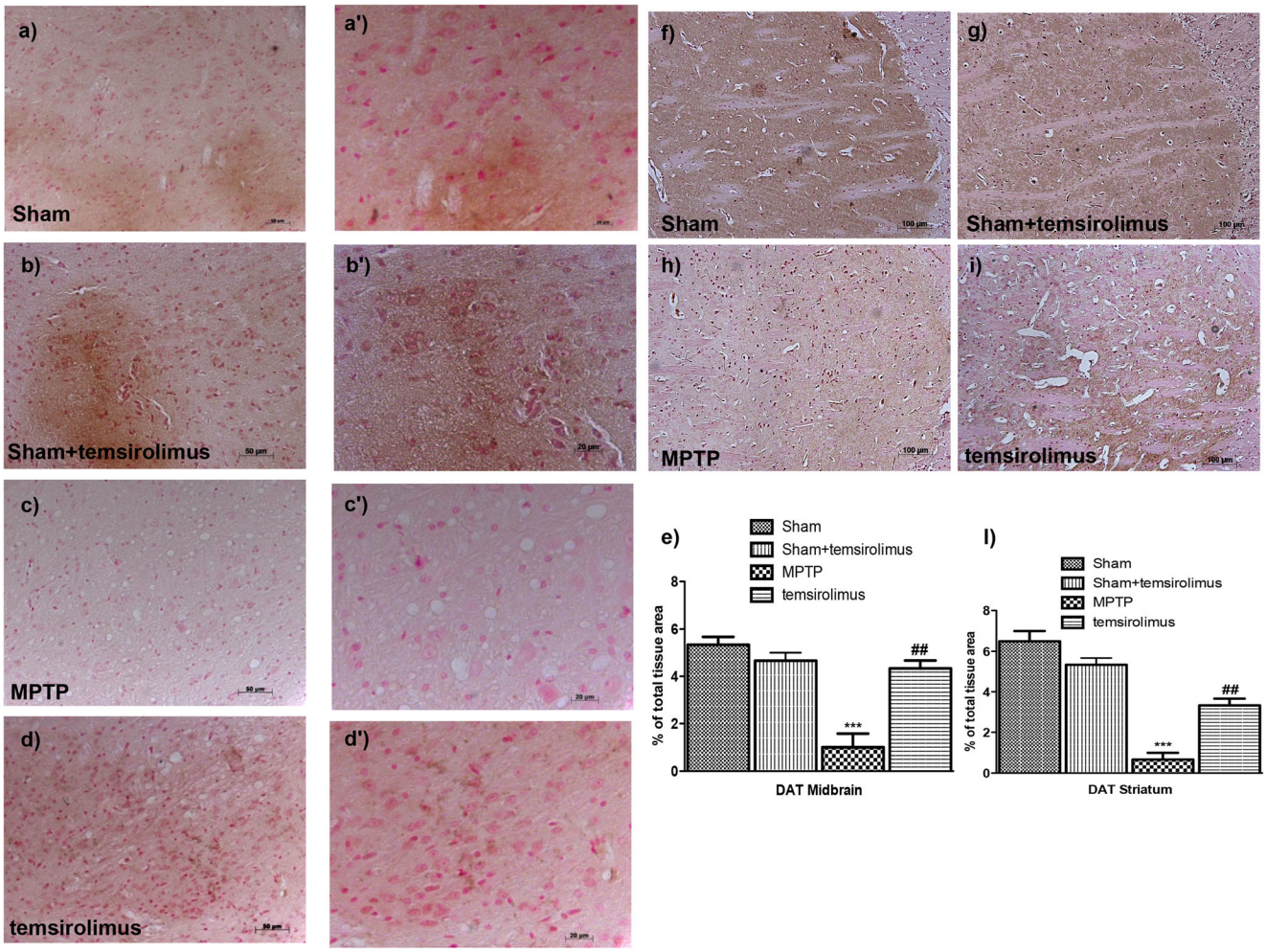

Fig. 3 Effects of temsirolimus on DAT expression in SN of MPTP-treated mice. Brain was stained with antibodies against DAT. Immunohistochemical analysis of midbrain obtained from mice after MPTP intoxication revealed a striking loss of DAT-positive cells (*c*, *c′* see densitometric analysis, *e*) compared with Sham and Sham+temsirolimus mice (*a*, *a′*; *b*, *b′* see densitometric analysis, *e*). Mice subjected to treatment with temsirolimus revealed a positive staining for DAT (*d*, *d′* see densitometric analysis, *e*). Immunohistochemical analysis of striatum obtained from mice after MPTP intoxication revealed a decline of DAT levels (*h* see densitometric analysis, *l*) compared with Sham and Sham+temsirolimus mice (*f*, *g* see densitometric analysis, *l*). Mice subjected to treatment with temsirolimus revealed a positive staining for DAT (*i* see densitometric analysis, *l*). Data are expressed as a percentage of total tissue area and are means ± SE of 5 mice/group. (*e*) ***$p < 0.001$ vs Sham and Sham+temsirolimus; ##$p < 0.01$ vs MPTP; (*l*) ***$p < 0.001$ vs Sham and Sham+temsirolimus; ##$p < 0.01$ vs MPTP

cytosolic fraction, that treatment with temsirolimus maintained high levels of LC3 (Fig. 6 d, and see relative densitometry analysis d′).

In a second step, to confirm the ability of temsilorimus to promote autophagy, the levels of specific proteins were determined by immunohistochemistry staining. We showed that a positive immunostaining for Beclin-1 was found in MPTP group at 8 days after MPTP-intoxication (Fig. 7 c, c′ and see relative densitometry analysis i). Temsirolimus-treated mice showed significantly increased of Beclin-1 immunoreactive cells in the SN (Fig. 7 d, d′ and see relative densitometry analysis i). On the contrary, we observed a positive immunostaining for mTOR in Sham, Sham+temsirolimus, and MPTP groups (Fig. 7 e, e′; f, f′; g, g′ and see relative densitometry analysis i), while treatment with temsirolimus significantly decreased mTOR expression in the MPTP+temsirolimus group (Fig. 7 h, h′ and see relative densitometry analysis i).

Finally, we wanted to assess whether the autophagy markers were upregulated in dopaminergic neurons. Wherefore, by immunofluorescence analysis, we demonstrated that TH, the specific marker of dopaminergic neurons, co-localized with Beclin-1 and mTOR that promote and inhibit autophagy, respectively.

Midbrain sections were double stained with anti-TH (green) and anti-Beclin-1 and anti-mTOR (red antibodies). Immunofluorescence revealed that TH was significantly lower in MPTP-injected mice (Fig. 8 g and j) compared to the sham group (Fig. 8 a and d). TH immunoreactivity was significantly increased in mice treated with temsirolimus (Fig. 8 m, and p).

Instead, Beclin-1 increased in a non-significant manner after MPTP-intoxication (Fig. 8 h); treatment with temsirolimus

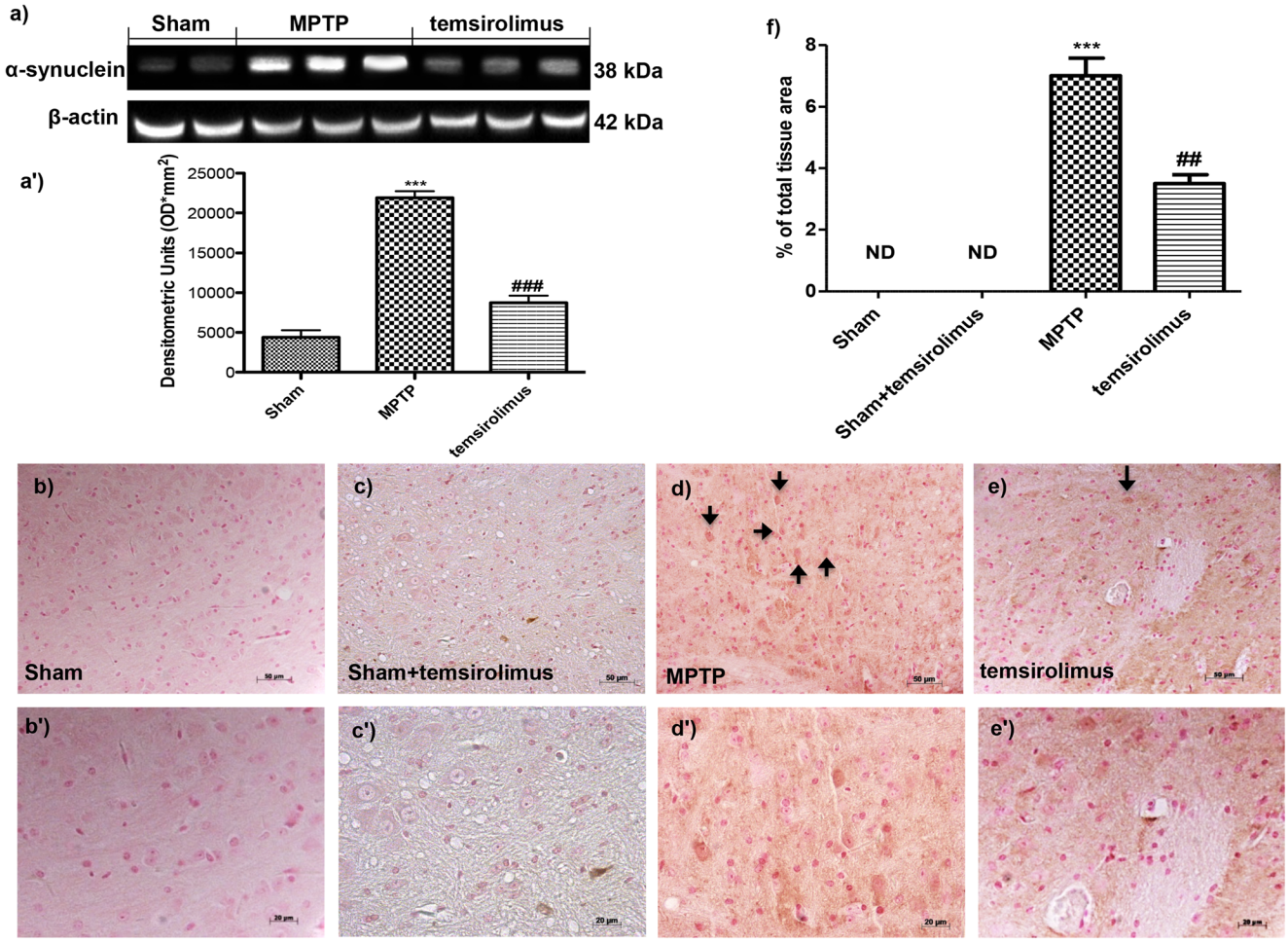

Fig. 4 Effects of temsirolimus on α-synuclein expression in SN of MPTP-treated mice. Midbrain was stained with antibodies against α-synuclein (*b*–*e*). Immunohistochemical analysis of midbrain obtained from mice subjected to MPTP intoxication revealed a positive staining for α-synuclein (*d*, *d*′ see densitometric analysis, *f*) compared with Sham mice (*b*, *b*′ see densitometric analysis, *f*) and Sham+temsirolimus group (*c*, *c*′ see densitometric analysis, *f*). The treatment with temsirolimus significantly reduced a positive staining for α-synuclein in the SN (*e*, *e*′ see densitometric analysis, *f*). Data are expressed as a percentage of total tissue area and are means ± SE of 5 mice/group. ***$p < 0.001$ vs Sham and Sham+temsirolimus; ##$p < 0.01$ vs MPTP. Western blot analysis in the cytosolic fraction confirmed our data (*a*, *a*′). Each data are expressed as mean ± SEM from $N = 5$ mice/group. ***$p < 0.001$ vs Sham; ###$p < 0.001$ vs MPTP (*a*′)

led to a significant increase in the expression of Beclin-1 (Fig. 8 n). On the contrary, mTOR, which inhibits autophagy, presented high levels in Sham and MPTP groups (Fig. 8 k), while mTOR immunoreactivity was significantly reduced following treatment with temsirolimus (Fig. 8 q). In both cases, there was a co-localization of TH with Beclin-1 and mTOR.

The yellow arrow indicates the co-localization between TH/Beclin-1 and TH/mTOR (Fig. 8 c, i, o and Fig. 8 f, l, r). The images above are representative of triplicate experiments. All images were scanned at a resolution of 8 bits in an array of 2048 × 2048 pixels.

Temsirolimus Treatment Reduces Astrocyte and Microglial Activation in Brain of MPTP Treated Mice

To investigate astrocyte and microglial activation in relation to PD pathology, Western blot analysis was applied to quantify the expression of GFAP and Iba-1. The GFAP and Iba-1 levels were low in the Sham group, but significantly elevated following treatment with MPTP. Under these conditions, temsirolimus treatment significantly reduced the increased expression of GFAP and Iba-1 (Fig. 9 a and b, see relative densitometry analysis a′ and b′).

Temsirolimus Restores MPTP-Induced Loss of Brain-Derived Neurotrophic Factor (BDNF) and Neurotrophins 3 (NT-3) Expression in Mice

The neurotrophins BDNF and NT-3 are important to support the survival of existing neurons and to promote the growth and differentiation of new neurons and synapses. To investigate whether temsirolimus modulates the inflammatory process through regulation of the neurotrophic factors levels, and to show their location in specific cell types, we performed

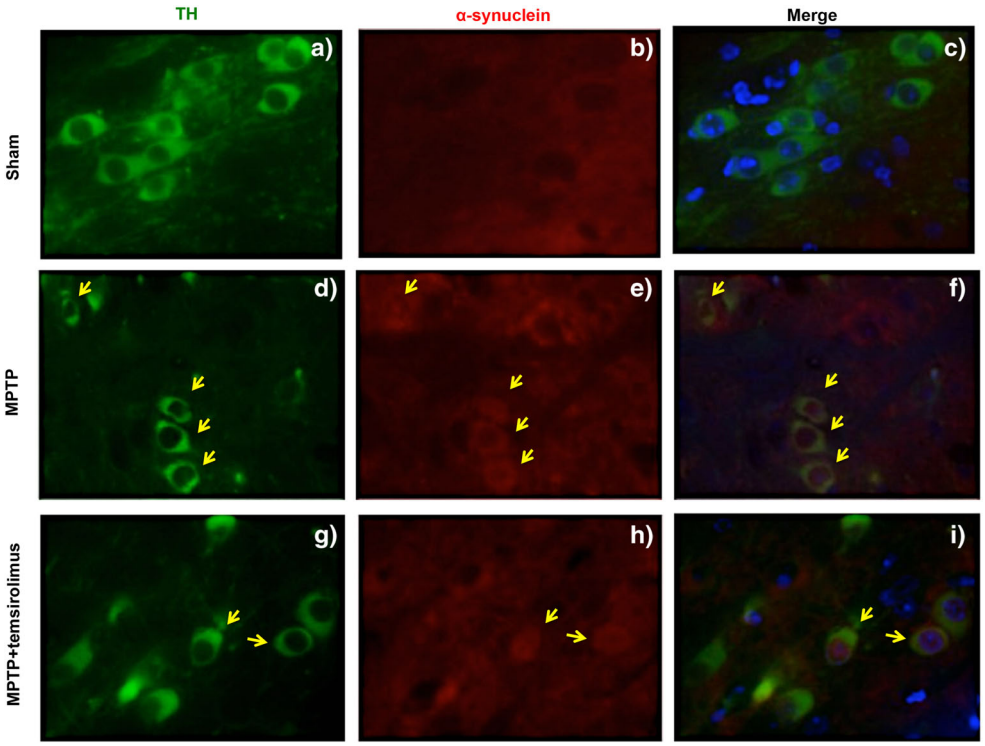

Fig. 5 Co-localization of TH/α-synuclein after MPTP-intoxication. Results are shown for (*a–c*) Sham group, (*d–f*) mice after MPTP-intoxication, (*g–i*) mice treated with temsirolimus. Midbrain sections were double stained with antibodies against TH (*a*, *d*, *g green*)/α-synuclein (*b*, *e*, *h red*). Midbrain sections revealed a decreased TH expression (*d*) and an increased of α-synuclein (*e*) in MPTP group. TH immunoreactivity was increased in temsirolimus-treated mice (*g*), while was decreased α-synuclein positive neurons. The pictures are demonstrative of at least three experiments executed on distinctive experimental days. Images are representative of all the animals in every group. All images were digitalized at a resolution of 8 bits into an array of 2048 × 2048 pixels. *Scale bar* 10 μm

immunofluorescence staining with Iba-1 and GFAP, microglial and astrocyte activation marker, respectively. Midbrain sections were double stained with antibodies against GFAP and Iba-1 (green) and BDNF and NT-3 (red). Immunofluorescence staining revealed that GFAP was significantly higher in MPTP-injected mice (Fig. 10 g and Fig. 11 g) such as activation of the microglia (Fig. 10 j and Fig. 11 j) than in the Sham group (Fig. 10 a, d and Fig. 11 a, d). GFAP and Iba-1 immunoreactivity were significantly reduced in mice treated with temsirolimus (Fig. 10 m, p and Fig. 11 m, p). On the contrary, the neurotrophic factors were decreased in animals after MPTP-intoxication (Fig. 10 h, k and Fig. 11 h, k), while treatment with temsirolimus significantly increased the release of BDNF and NT-3 (Fig. 10 n, q and Fig. 11 n, q). The yellow arrow indicates the co-localization between BDNF and GFAP (Fig. 10 o) and NT-3 and GFAP (Fig. 11 o) as well as between BDNF and Iba-1 (Fig. 10 r), and NT-3 and Iba-1 (Fig. 11 r). Reported images are representative of triplicate experiments. All images were digitalized at a resolution of 8 bits into an array of 2048 × 2048 pixels.

Temsirolimus Modulates Expression of p-JNK, p38, and p-ERK after MPTP-Intoxication

The MAPKs are a family of evolutionally conserved molecules playing a critical role in cell signaling and gene expression. MAPKs family includes three major members: extracellular signal-regulated kinase (ERK), p38, and c-Jun N-terminal kinase (JNK), representing three different signaling cascades [42]. To determine that treatment with temsirolimus modulates the expression of these MAPKs, we performed Western blot analysis in the cytosolic fraction. Low expression of p-JNK, p-p38, and p-ERK was detected in brain samples from mice sham, while levels of these MAPKs were considerably increased in mice after MPTP-intoxication. As indicated by densitometry analysis, temsirolimus decreased significantly the expression of p-JNK, p-p38, and p-ERK (Fig. 12 a, b and c, see relative densitometry analysis a′, b′, and c′).

Discussion

The most common neurodegenerative diseases, such as AD, PD, HD, and amyotrophic lateral sclerosis (ALS), are characterized by toxic protein aggregates and damaged organelles that accumulate inside specific types of neurons and cause neuronal dysfunction and ultimately neuronal death. In particular, PD caused the selective cell death of dopaminergic neurons in the SN and is characterized by the presence of Lewy bodies containing α-synuclein aggregates [43].

Recently, there is a growing interest for the role of autophagy pathways in neurodegenerative diseases. Autophagy is a lysosomal degradative pathway that is implicated in regulating cellular response to stress and is crucial for the clearance of toxic substances from cells in specific areas of the brain, thereby exerting a neuroprotective and/or neurodegenerative properties [44, 45]. Under basal conditions, autophagic activity is low but can be activated by physiological and pathological

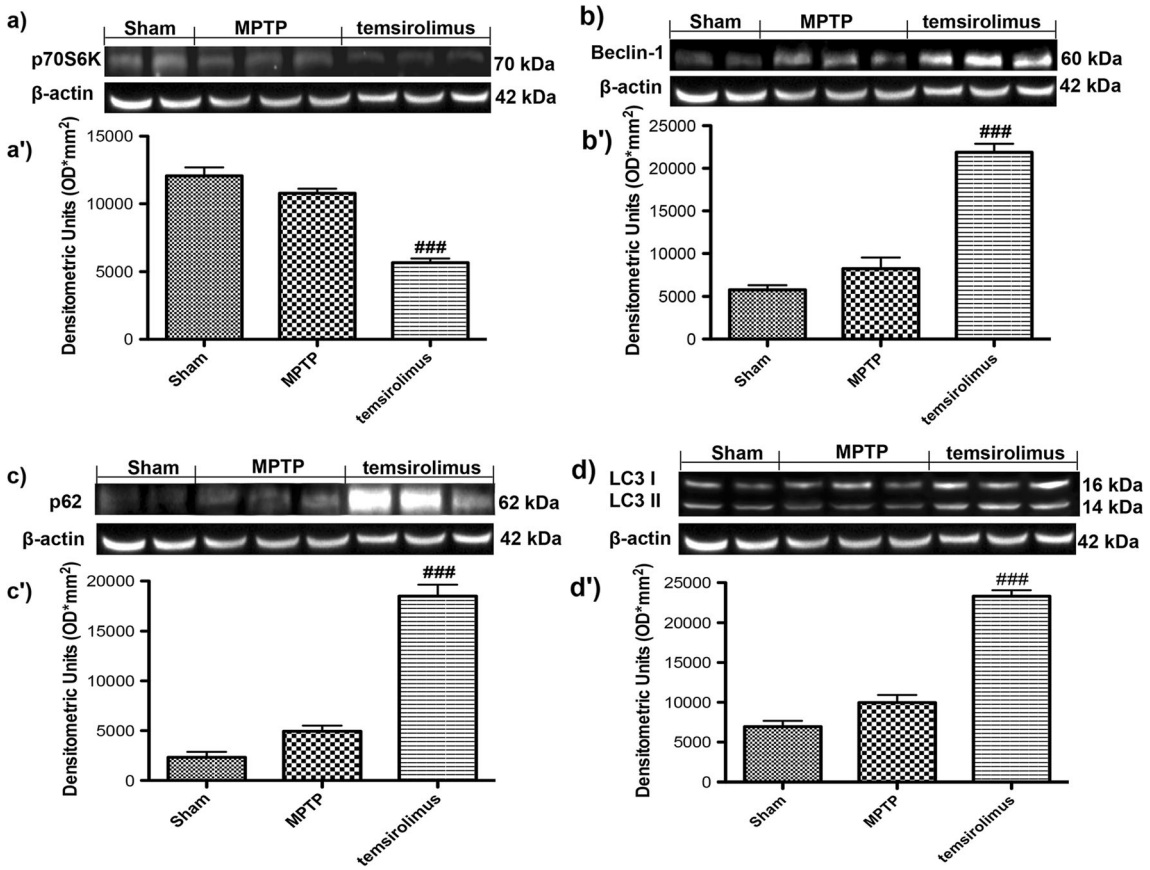

Fig. 6 Effect of temsirolimus on autophagy process after MPTP intoxication. Western blot analysis for p70S6K in the cytosolic fraction showed that after MPTP-intoxication the levels of p70S6K decreased (*a*, *a*′), while treatment with temsirolimus significantly reduced the levels of p70S6K (*a*, *a*′). Western blot analysis for Beclin-1, p62, and LC3 in the cytosolic fraction showed that MPTP intoxication elevated levels of these proteins (*b*, *b*′; *c*, *c*′; *d*, *d*′). Treatment with temsirolimus significantly maintained high levels of Beclin-1, p62, and LC3 (*b*, *b*′; *c*, *c*′; *d*, *d*′). Data are representative of at least three independent experiments. Data are expressed as mean ± SEM from $N = 5$ mice/group. ###$p < 0.001$ vs MPTP (*a*′; *b*′; *c*′; *d*′)

conditions in multiple organs. Thus, autophagic and proteosomal degradation pathways have been proposed to mediate α-synuclein clearance [46]. It has been demonstrated that rapamycin, a molecule able to activating autophagy process, exerts neuroprotective effects in PD models [33, 47]. However, rapamycin has important side effects; thus based on these evidences, we evaluated an analogous of rapamycin, temsirolimus, in in vivo models of PD. It has been known that PD affecting dopaminergic neurons causes significant decrease on locomotor activity, thus first of all we analyzed, with two different tests, the recovery of motor behavioral functions: rotarod test and catalepsy test. At 8 days after MPTP intoxication, vehicle-treated animals showed considerable motor deficits revealed by reducing the time spent on the rotarod and by a significantly increased cataleptic response in the catalepsy test. Treatment with temsirolimus markedly enhanced motor and behavioral function in both tests. Although recognized as the most widespread neurodegenerative motor pathology, PD is accompanied by a number of non-motor symptoms (particularly psychiatric features), which generally receive less attention, but represent a major challenge in the treatment of PD [48]. In order to evaluate the depression-like behavior in PD rodent models and the effect of temsirolimus on these aspects of PD, we utilized the FST and EPM behavioral tests. MPTP administration determinate increased immobility in the FST and anxiety in EPM, whereas treatment with temsirolimus reversed MPTP-induced immobility and anxiety. PD is also characterized by Lewy bodies inclusion that are largely composed of the protein α-synuclein that is a crucial marker of PD pathogenesis. Thus, in this study we evaluated the amount and the aggregation of α-synuclein and we observed that α-synuclein significantly increased in the brain taken from mice treated with MPTP compared to sham group, while temsirolimus administration induced an important reduction of α-synuclein aggregates. Another important features in PD initiation and progression is the alteration of dopamine production that we identified with the specific markers TH, that is the enzyme responsible for catalyzing the conversion of the amino acid L-tyrosine into dihydroxyphenylalanine (DOPA), a precursor for dopamine,

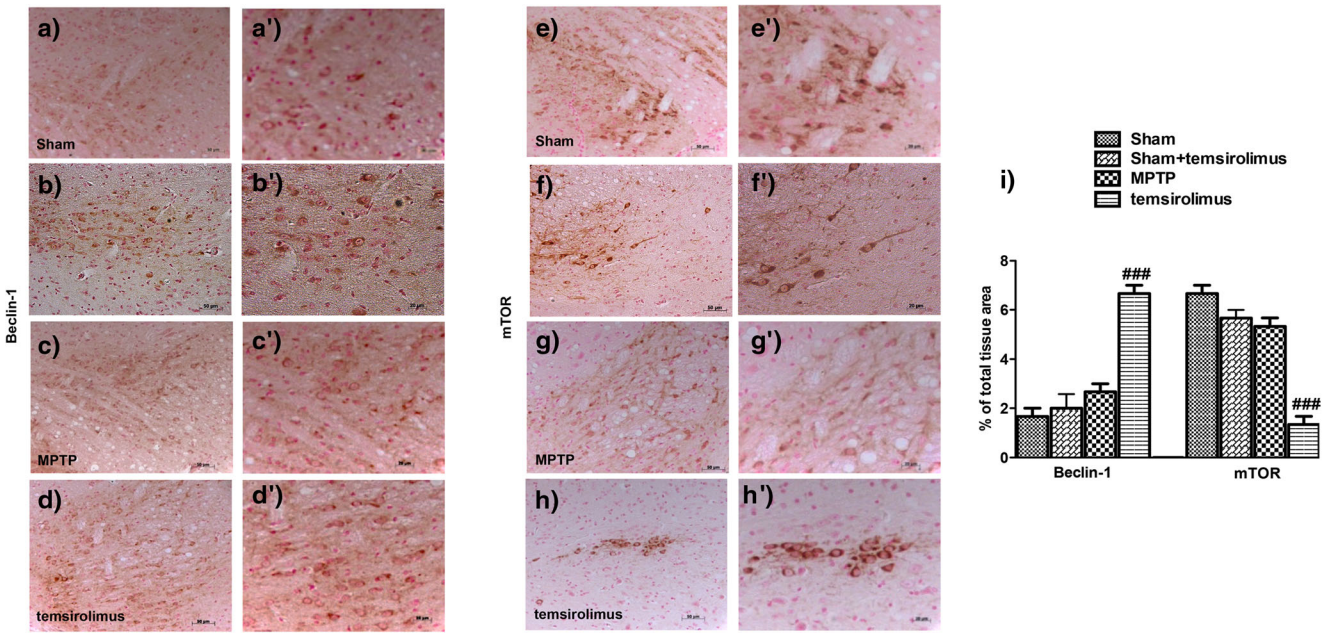

Fig. 7 Effect of temsirolimus on Beclin-1 and mTOR expression. By immunohistochemical analysis, a low level of Beclin-1 positive staining was detected in midbrain samples from Sham, Sham+temsirolimus, and MPTP groups (*a*, *a′*; *b*, *b′*; *c*, *c′* see densitometric analysis, *i*). Beclin-1 expression was significantly increased in midbrain samples from mice treated with temsirolimus (*d*, *d′* see densitometric analysis, *i*). While this analysis for mTOR showed a high positive immunostaining in Sham, Sham+temsirolimus, and MPTP groups (*e*, *e′*; *f*, *f′*; *g*, *g′* see densitometric analysis, *i*), while mTOR expression significantly decreased in mice treated with temsirolimus (*h*, *h′* see densitometric analysis, *i*). Data are expressed as a percentage of total tissue area and are means ± SE of 5 mice/group. ###$p < 0.001$ vs MPTP

and DAT, a member of a large family of $Na^{+}Cl^{-}$-dependent transporters, which is thought to control the synaptic activity of released dopamine by rapid reuptake of the neurotransmitter into presynaptic terminals.

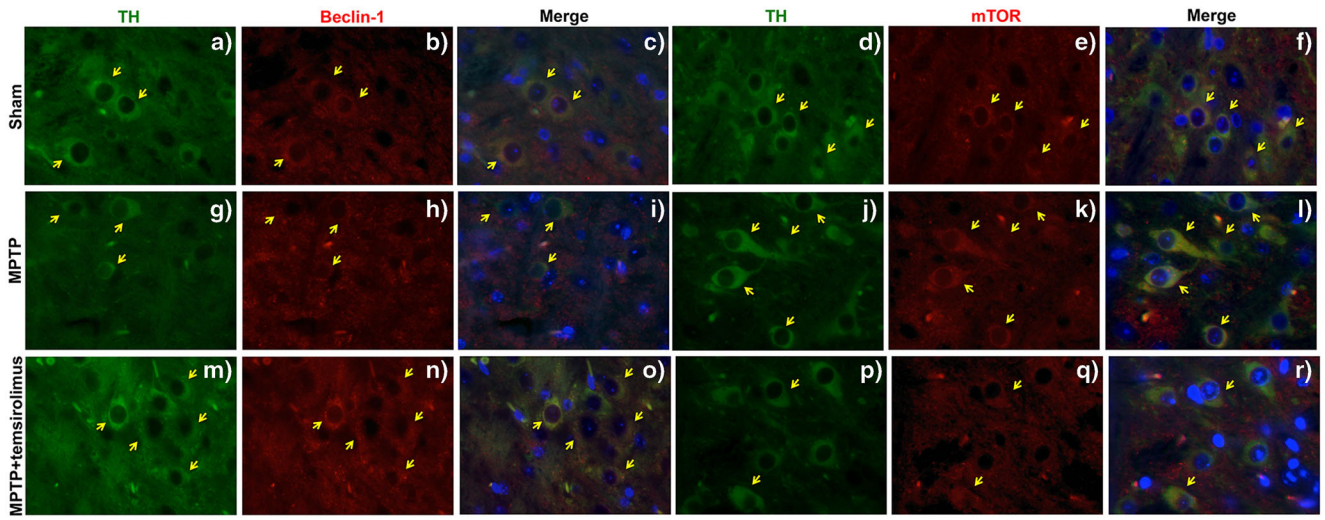

Fig. 8 Co-localization of TH/Beclin-1 and TH/mTOR after MPTP-intoxication. Results are shown for (*a–c*, *d–f*) sham group, (*g–i*, *j–l*) mice after MPTP-intoxication, and (*m–o*, *p–r*) mice treated with temsirolimus. Midbrain sections were double stained with antibodies against TH (*a*, *g*, *m green*)/Beclin-1 (*b*, *h*, *n red*), and TH (*d*, *j*, *p green*)/mTOR (*e*, *k*, *q red*). Midbrain sections revealed decreased TH in MPTP group (*g*, *j*). TH immunoreactivity was increased in temsirolimus-treated mice (*m*, *p*). Moreover, Beclin-1 and mTOR expression remained almost at the levels of the control groups (*h*, *k*), while treatment with temsirolimus significantly increased the levels of Beclin-1 (*n*) and decreased mTOR expression (*q*) Yellow spots indicate co-localizations and revealed a high co-localization between TH/Beclin-1 and TH/mTOR double staining. The pictures are demonstrative of at least three experiments executed on distinctive experimental days. Images are representative of all the animals in every group. All images were digitalized at a resolution of 8 bits into an array of 2048 × 2048 pixels. *Scale bar* 10 μm

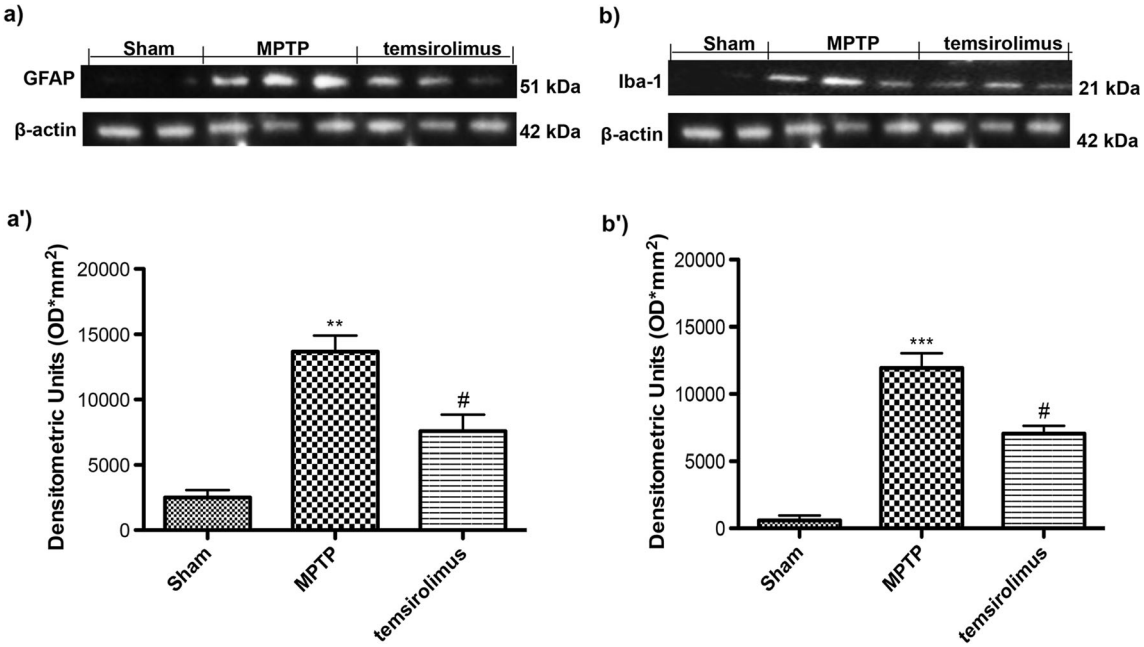

Fig. 9 Effect of temsirolimus on GFAP and Iba-1 expression after MPTP intoxication. Western blot analysis for GFAP and Iba-1 in the cytosolic fraction showed an increase of levels of these proteins in MPTP group compared to the Sham group, while the treatment with temsirolimus significantly reduced GFAP and Iba-1 levels (*a*, *a*′; *b*, *b*′, respectively). The data are representative of at least three independent experiments. Each data are expressed as mean ± SEM from $N = 5$ mice/group. $^{**}p < 0.01$ vs Sham; $\#p < 0.05$ vs MPTP (*a*); $^{**}p < 0.01$ vs Sham; $\#p < 0.05$ vs MPTP (*b*)

In the present study, we showed that treatment with temsirolimus attenuated significantly the loss of TH and DAT induced by the administration of MPTP. Moreover, stereology analysis confirmed that treatment with temsirolimus significantly increased the number of TH-positive cells, compared with the MPTP group, indicating that temsirolimus has the ability to prevent the degeneration of dopaminergic neurons in this mouse model of PD.

There is increasing interest in the role of autophagy in regulating the pathophysiology process of PD and in particular the clearance of α-synuclein [49]. Autophagy inhibition is often connected with sure diseases, as well as a subset of

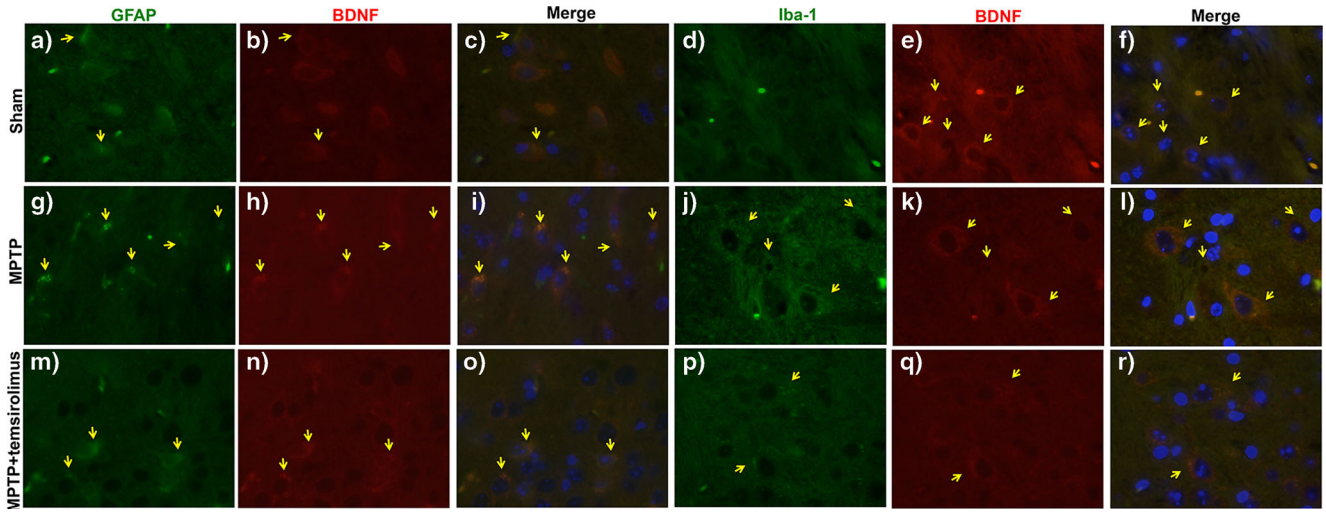

Fig. 10 Co-localization of GFAP/BDNF and Iba-1/BDNF after MPTP-intoxication. Results are shown for (*a–c*, *d–f*) sham group, (*g–i*, *j–l*) mice after MPTP-intoxication, and (*m–o*, *p–r*) mice treated with temsirolimus (*m–o*, *p–r*). Midbrain sections were double stained with antibodies against GFAP (*a*, *g*, *m green*), Iba-1 (*d*, *j*, *p green*), and BDNF (*b*, *h*, *n*, *e*, *k*, *q red*). Midbrain sections revealed increased astrogliosis (GFAP+ cells) (*g*) and microgliosis (Iba-1+ cells) (*j*) in MPTP group. GFAP and Iba-1 immunoreactivity was reduced in temsirolimus-treated mice (*m*, *p*). *Yellow spots* indicate co-localizations and revealed a high co-localization between GFAP/BDNF and Iba-1/BDNF double staining. The pictures are demonstrative of at least three experiments executed on distinctive experimental days. Images are representative of all the animals in every group. All images were digitalized at a resolution of 8 bits into an array of 2048 × 2048 pixels. *Scale bar* 10 μm

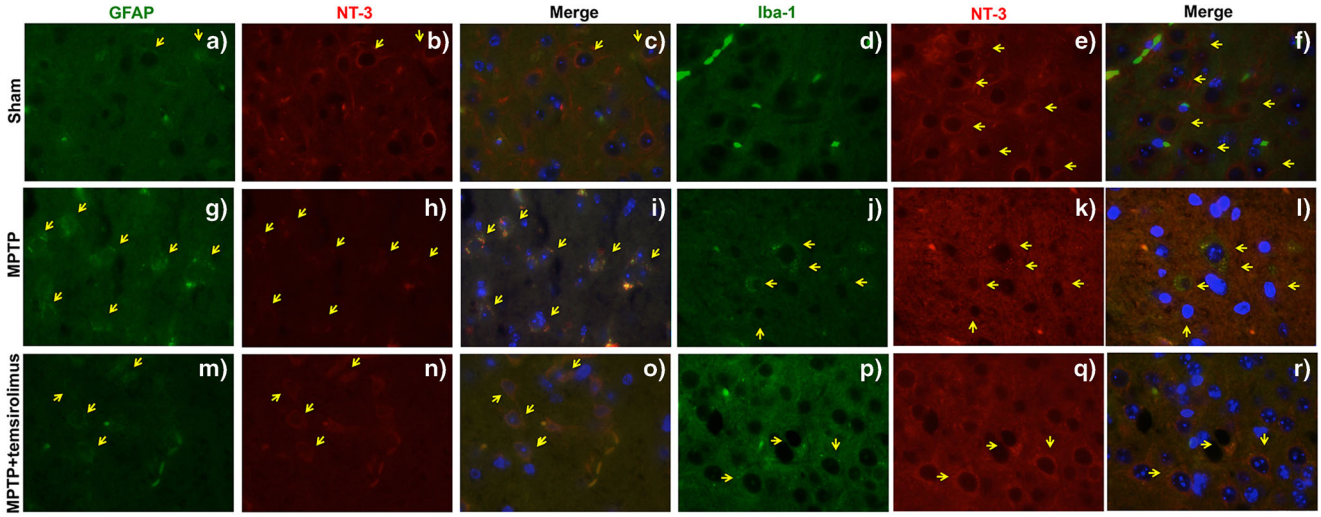

Fig. 11 Co-localization of GFAP/NT-3 and Iba-1/NT-3 after MPTP -intoxication. Results are shown for (*a–c*, *d–f*) sham group, (*g–i*, *j–l*) mice after MPTP-intoxication, and (*m–o*, *p–r*) mice treated with temsirolimus (*m–o*, *p–r*). Midbrain sections were double stained with antibodies against GFAP (*a*, *g*, *m green*), Iba-1 (*d*, *j*, *p green*), and NT-3 (*b*, *h*, *n*, *e*, *k*, *q red*). Midbrain sections revealed increased astrogliosis (GFAP+ cells) (*g*) and microgliosis (Iba-1+ cells) (*j*) in MPTP group. GFAP and Iba-1 immunoreactivity was reduced in temsirolimus-treated mice (*m*, *p*). *Yellow spots* indicate co-localizations and revealed a high co-localization between GFAP/NT-3 and Iba-1/NT-3 double staining. The pictures are demonstrative of at least three experiments executed on distinctive experimental days. Images are representative of all the animals in every group. All images were digitalized at a resolution of 8 bits into an array of 2048 × 2048 pixels. *Scale bar* 10 μm

cancers, neurodegenerative disorders, infectious diseases, and inflammatory bowel disorders [16, 50]. The regulation of autophagy seems to converge on the enzyme mTOR, a kinase that activates protein synthesis and simultaneously inhibits autophagy, acting as a checkpoint with upstream Akt and downstream p70S6K—the two most important mediators [51]. In our study, we observed a basal level for mTOR in Sham and MPTP groups, while treatment with temsirolimus significantly decreased mTOR expression that is correlated with the reduced levels of p70S6K, autophagy protein promoter, that was kept low by the administration of temsirolimus, thus resulting in the stimulation of autophagy process.

It is known that the initiation step of autophagosome formation requires the Beclin1-class III PI3K complex, which contains Beclin1, Vps34 (class III PI3K), and p150 [52]. In fact, Beclin-1 binds to LC3I, which is then cleaved and converted to a membrane-associated form LC3-II through conjugating with the lipid PE [53]. LC3-II, the cleaved product of LC3-I, is inserted within the inner and outer membrane of the vesicles during autophagosome formation. LC3 then binds to the adaptor protein p62 sequestrome, which facilitates the autophagic degradation of ubiquitinated protein aggregates in lysosomes. In this study, we found that Beclin-1, p62, and LC3 expression were slightly higher in the MPTP group, while treatment with temsirolimus leads to a significant increase in the expression of these proteins stimulating in turn the autophagy process.

After proving that temsirolimus was able to inhibit mTOR and really activate autophagy, our objective was to evaluate the importance of this process in dopaminergic neurons. In particular, we wanted to demonstrate if proteins involved in autophagy, such as Beclin-1 and mTOR, were upregulated by dopaminergic neurons. For this reason, using immunofluorescence analysis, we demonstrated that there is the co-localization of TH with Beclin-1 and mTOR that promote and inhibit autophagy, respectively.

It has been know that neurotrophins such as BDNF and NT-3 play an important role in the functionality of neurons and its levels are significantly reduced in PD [54]. Based on of these evidences, we evaluated the activity of temsirolimus in limiting neurotrophins degradation, so we have shown by immunofluorescence staining that levels of BDNF and NT-3 were reduced in mice group MPTP, while temsirolimus treatment increased the expression of these neurotrophins in significant ways [5, 55, 56]. The inflammation of neurons causes release of various inflammatory mediators (IFNs, EGF, IL5, IL6, HGF, LIF, and BMP2). Key features of neuroinflammation [5, 57] are closely associated in the brain with activation of astrocytes and microglia and with the increased production of cytokines, chemokines, prostaglandins, complement cascade proteins, and reactive oxygen and nitrogen species (ROS/RNS) which in some cases can result in disruption of the blood brain barrier and direct participation of the adaptive immune system [58]. Furthermore, several preclinical and some clinical studies have revealed that the mTOR overactivation produces brain abnormalities, abnormal cortical organization, and astrogliosis. mTOR inhibitors (e.g., rapamycin) have consistent protective effects in various genetic (e.g., TSC models and WAG/Rij rats) and acquired (e.g., kainate or pilocarpine post-status epilepticus) epilepsy animal models and other neurological disorders [59–61]. In the

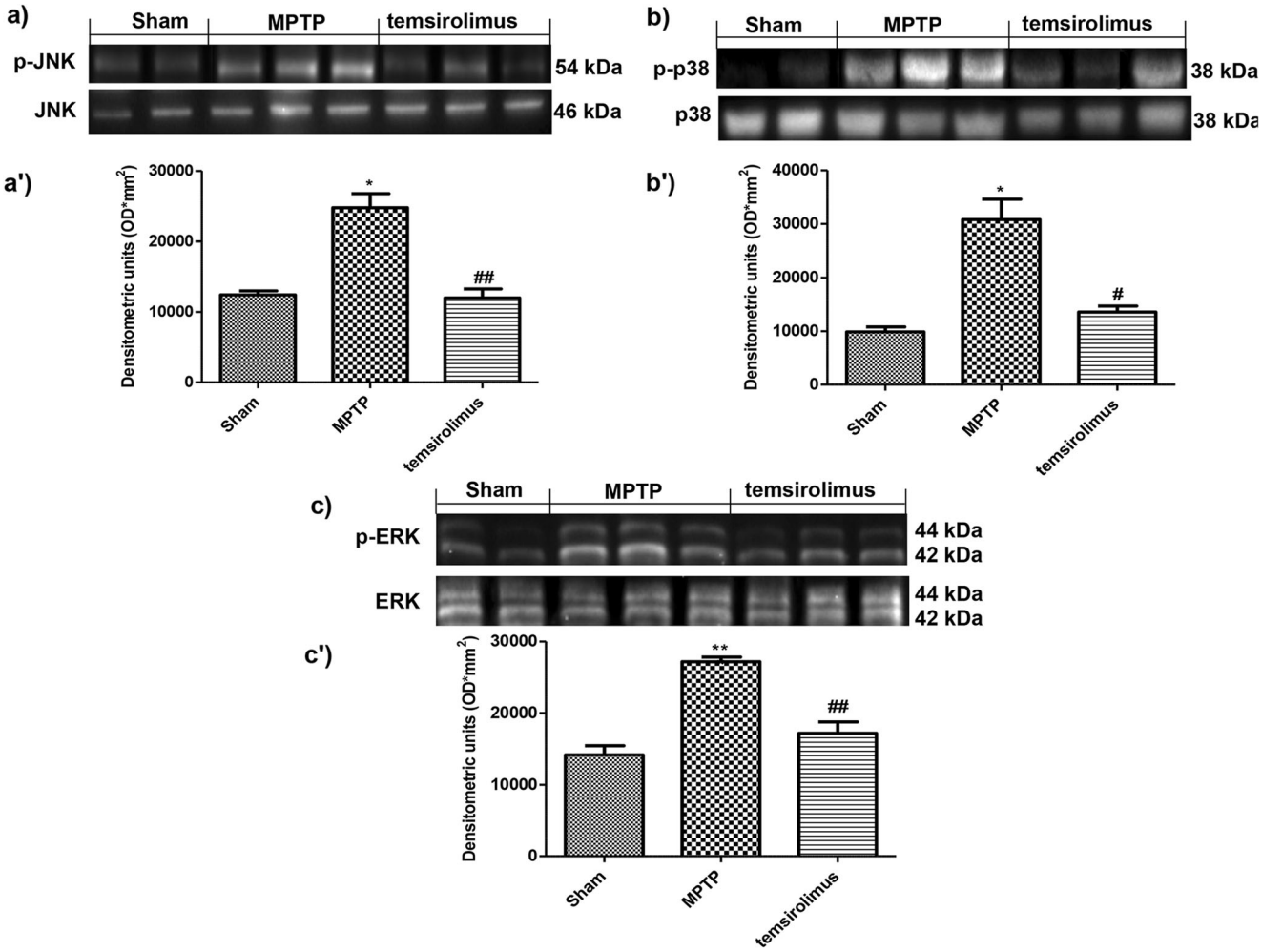

Fig. 12 Effect of temsirolimus on MAPKs pathway after MPTP intoxication. Western blot analysis for p-JNK, p-p38, and p-ERK in the cytosolic fraction showed an increase of levels of these proteins in MPTP group compared to the Sham group, while the treatment with temsirolimus significantly reduced p-JNK, p-p38, and p-ERK expression (*a*, *a*′; *b*, *b*′; *c*, *c*′, respectively). The data are representative of at least three independent experiments. Each data are expressed as mean ± SEM from $N = 5$ mice/group. *$p < 0.05$ vs Sham; ##$p < 0.01$ vs MPTP (*a*′); *$p < 0.005$ vs Sham; #$p < 0.05$ vs MPTP (*b*′); **$p < 0.01$ vs Sham; ##$p < 0.01$ vs MPTP (*c*′)

present study we observed that changes in GFAP and Iba-1 expression have been reported during brain damage or central nervous system degeneration, while temsirolimus significantly prevented both astrogliosis and microgliosis. Thus targeting neuroinflammation could be one intervention that can slow down the progression of PD. Moreover, emerging evidence suggests that oxidative stress participates in the loss of nigral neurons in PD [47], oxidative stress response that is mediated by the activation of a cascade of MAPKs. The family MAPK phosphorylates serine and specific threonine substrates target proteins and regulate cellular activities such as survival, proliferation, differentiation, and apoptosis [62, 63]. Therefore, to clarify the molecular and cellular mechanisms underlying the ability of neuronal recovery, we assessed the modulation of MAPK by temsirolimus. In this study, we found that MPTP induces the activation of the p-JNK, p-p38, and p-ERK signaling pathway in dopaminergic neurons, while in the brain sections from mice treated with temsirolimus the expression of these proteins were decreases.

Our results clearly demonstrate the several functions of temsirolimus. In fact, this compound is able to improve neurobehavioral functions, the integrity of the neuronal tissue with consequent reduction of the cell death, and to modulate the neuroinflammatory pathway involved in PD. Furthermore, in the present study we confirmed the crucial role of autophagy in modulating the PD pathogenesis highlighting how treatment with temsirolimus clearly stimulates autophagy protecting from loss of cells and α-synuclein toxicity in neuronal PD. Therefore, understanding the neuronal autophagy process will ultimately aid in drug target identification and rational design of drug screening to counteract neurodegenerative diseases. Thus, our observations indicate that temsirolimus may be considered as a new therapeutic target to improve neurodegenerative disorders such as PD.

Acknowledgements The authors would like to thank Maria Antonietta Medici for her excellent technical assistance during this study and Mr. Francesco Soraci for his secretarial and administrative assistance and Miss Valentina Malvagni for her editorial assistance with the manuscript.

Compliance with Ethical Standards The study was approved by the University of Messina Review Board for the care of animals. All animal experiments complied with regulations in Italy (D.M. 116192) as well as the EU regulations (O.J. of E.C. L 358/1 12/18/1986).

Conflict of Interest The authors declare that they have no conflict of interest.

References

1. Moore DJ, West AB, Dawson VL, Dawson TM (2005) Molecular pathophysiology of Parkinson's disease. Annu Rev Neurosci 28: 57–87. doi:10.1146/annurev.neuro.28.061604.135718
2. Sulzer D, Surmeier DJ (2013) Neuronal vulnerability, pathogenesis, and Parkinson's disease. Movement disorders : official journal of the Movement Disorder Society 28(1):41–50. doi:10.1002/mds.25095
3. Dauer W, Przedborski S (2003) Parkinson's disease: mechanisms and models. Neuron 39(6):889–909
4. Marras C, Lang A (2008) Invited article: changing concepts in Parkinson disease: moving beyond the decade of the brain. Neurology 70(21):1996–2003. doi:10.1212/01.wnl.0000312515.52545.51
5. Hirsch EC, Hunot S (2009) Neuroinflammation in Parkinson's disease: a target for neuroprotection? Lancet Neurol 8(4):382–397. doi:10.1016/S1474-4422(09)70062-6
6. Mehta SH, Tanner CM (2016) Role of neuroinflammation in Parkinson disease: the enigma continues. Mayo Clin Proc 91(10): 1328–1330. doi:10.1016/j.mayocp.2016.08.010
7. Mitra S, Ghosh N, Sinha P, Chakrabarti N, Bhattacharyya A (2016) Alteration of nuclear factor-kappaB pathway promote neuroinflammation depending on the functions of estrogen receptors in substantia nigra after 1-methyl-4-phenyl-1,2,3,6-tetrahydropyridine treatment. Neurosci Lett 616:86–92. doi:10.1016/j.neulet.2016.01.046
8. Lee HJ, Kim C, Lee SJ (2010) Alpha-synuclein stimulation of astrocytes: potential role for neuroinflammation and neuroprotection. Oxidative Med Cell Longev 3(4):283–287. doi:10.4161/oxim.3.4.12809
9. Xilouri M, Brekk OR, Stefanis L (2016) Autophagy and alpha-synuclein: relevance to Parkinson's disease and related synucleopathies. Movement disorders : official journal of the Movement Disorder Society 31(2):178–192. doi:10.1002/mds.26477
10. de Oliveira RM, Vicente Miranda H, Francelle L, Pinho R, Szego EM, Martinho R, Munari F, Lazaro DF et al (2017) The mechanism of sirtuin 2-mediated exacerbation of alpha-synuclein toxicity in models of Parkinson disease. PLoS Biol 15(3):e2000374. doi:10.1371/journal.pbio.2000374
11. Redmann M, Wani WY, Volpicelli-Daley L, Darley-Usmar V, Zhang J (2017) Trehalose does not improve neuronal survival on exposure to alpha-synuclein pre-formed fibrils. Redox Biol 11: 429–437. doi:10.1016/j.redox.2016.12.032
12. Levine B, Klionsky DJ (2004) Development by self-digestion: molecular mechanisms and biological functions of autophagy. Dev Cell 6(4):463–477
13. Wang C, Liang CC, Bian ZC, Zhu Y, Guan JL (2013) FIP200 is required for maintenance and differentiation of postnatal neural stem cells. Nat Neurosci 16(5):532–542. doi:10.1038/nn.3365
14. Yue Z, Friedman L, Komatsu M, Tanaka K (2009) The cellular pathways of neuronal autophagy and their implication in neurodegenerative diseases. Biochim Biophys Acta 1793(9):1496–1507. doi:10.1016/j.bbamcr.2009.01.016
15. Hu X, Song Q, Li X, Li D, Zhang Q, Meng W, Zhao Q (2017) Neuroprotective effects of Kukoamine A on neurotoxin-induced Parkinson's model through apoptosis inhibition and autophagy enhancement. Neuropharmacology 117:352–363. doi:10.1016/j.neuropharm.2017.02.022
16. Webb JL, Ravikumar B, Atkins J, Skepper JN, Rubinsztein DC (2003) Alpha-Synuclein is degraded by both autophagy and the proteasome. J Biol Chem 278(27):25009–25013. doi:10.1074/jbc.M300227200
17. Hu Q, Wang G (2016) Mitochondrial dysfunction in Parkinson's disease. Translational neurodegeneration 5:14. doi:10.1186/s40035-016-0060-6
18. Ouyang L, Zhang L, Liu B (2016) Autophagy pathways and key drug targets in Parkinson's disease. Yao xue xue bao = Acta pharmaceutica Sinica 51(1):9–17
19. Switon K, Kotulska K, Janusz-Kaminska A, Zmorzynska J, Jaworski J (2016) Molecular neurobiology of mTOR. Neuroscience. doi:10.1016/j.neuroscience.2016.11.017
20. Sabers CJ, Martin MM, Brunn GJ, Williams JM, Dumont FJ, Wiederrecht G, Abraham RT (1995) Isolation of a protein target of the FKBP12-rapamycin complex in mammalian cells. J Biol Chem 270(2):815–822
21. Pong K, Zaleska MM (2003) Therapeutic implications for immunophilin ligands in the treatment of neurodegenerative diseases. Curr Drug Targets CNS Neurol Disord 2(6):349–356
22. Radad K, Moldzio R, Rausch WD (2015) Rapamycin protects dopaminergic neurons against rotenone-induced cell death in primary mesencephalic cell culture. Folia Neuropathol 53(3):250–261. doi:10.5114/fn.2015.54426
23. Sola E, Lopez V, Burgos D, Cabello M, Gutierrez C, Martin A, Pena M, Gonzalez-Molina M (2006) Pulmonary toxicity associated with sirolimus treatment in kidney transplantation. Transplant Proc 38(8):2438–2440. doi:10.1016/j.transproceed.2006.08.037
24. Vlahakis NE, Rickman OB, Morgenthaler T (2004) Sirolimus-associated diffuse alveolar hemorrhage. Mayo Clin Proc 79(4): 541–545. doi:10.4065/79.4.541
25. Alkhatib AA (2006) Sirolimus-induced intractable chronic diarrhea: a case report. Transplant Proc 38(5):1298–1300. doi:10.1016/j.transproceed.2006.02.123
26. Altomare JF, Smith RE, Potdar S, Mitchell SH (2006) Delayed gastric ulcer healing associated with sirolimus. Transplantation 82(3):437–438. doi:10.1097/01.tp.0000228900.24951.66
27. Rubinsztein DC, Codogno P, Levine B (2012) Autophagy modulation as a potential therapeutic target for diverse diseases. Nat Rev Drug Discov 11(9):709–730. doi:10.1038/nrd3802
28. Yazbeck VY, Buglio D, Georgakis GV, Li Y, Iwado E, Romaguera JE, Kondo S, Younes A (2008) Temsirolimus downregulates p21 without altering cyclin D1 expression and induces autophagy and synergizes with vorinostat in mantle cell lymphoma. Exp Hematol 36(4):443–450. doi:10.1016/j.exphem.2007.12.008
29. Cortes CJ, La Spada AR (2014) The many faces of autophagy dysfunction in Huntington's disease: from mechanism to therapy. Drug Discov Today 19(7):963–971. doi:10.1016/j.drudis.2014.02.014
30. Jiang T, Yu JT, Zhu XC, Zhang QQ, Cao L, Wang HF, Tan MS, Gao Q et al (2014) Temsirolimus attenuates tauopathy in vitro and in vivo by targeting tau hyperphosphorylation and autophagic clearance. Neuropharmacology 85:121–130. doi:10.1016/j.neuropharm.2014.05.032

31. Graziani EI (2009) Recent advances in the chemistry, biosynthesis and pharmacology of rapamycin analogs. Nat Prod Rep 26(5):602–609. doi:10.1039/b804602f
32. Bozec A, Etienne-Grimaldi MC, Fischel JL, Sudaka A, Toussan N, Formento P, Milano G (2011) The mTOR-targeting drug temsirolimus enhances the growth-inhibiting effects of the cetuximab-bevacizumab-irradiation combination on head and neck cancer xenografts. Oral Oncol 47(5):340–344. doi:10.1016/j.oraloncology.2011.02.020
33. Malagelada C, Jin ZH, Jackson-Lewis V, Przedborski S, Greene LA (2010) Rapamycin protects against neuron death in in vitro and in vivo models of Parkinson's disease. J Neurosci 30(3):1166–1175. doi:10.1523/JNEUROSCI.3944-09.2010
34. Esposito E, Impellizzeri D, Mazzon E, Paterniti I, Cuzzocrea S (2012) Neuroprotective activities of palmitoylethanolamide in an animal model of Parkinson's disease. PLoS One 7(8):e41880. doi:10.1371/journal.pone.0041880
35. Heeneman S, Sluimer JC, Daemen MJ (2007) Angiotensin-converting enzyme and vascular remodeling. Circ Res 101(5):441–454. doi:10.1161/CIRCRESAHA.107.148338
36. Lee KW, Zhao X, Im JY, Grosso H, Jang WH, Chan TW, Sonsalla PK, German DC et al (2012) Apoptosis signal-regulating kinase 1 mediates MPTP toxicity and regulates glial activation. PLoS One 7(1):e29935. doi:10.1371/journal.pone.0029935
37. Fleming SM, Mulligan CK, Richter F, Mortazavi F, Lemesre V, Frias C, Zhu C, Stewart A et al (2011) A pilot trial of the microtubule-interacting peptide (NAP) in mice overexpressing alpha-synuclein shows improvement in motor function and reduction of alpha-synuclein inclusions. Mol Cell Neurosci 46(3):597–606. doi:10.1016/j.mcn.2010.12.011
38. Araki T, Kumagai T, Tanaka K, Matsubara M, Kato H, Itoyama Y, Imai Y (2001) Neuroprotective effect of riluzole in MPTP-treated mice. Brain Res 918(1–2):176–181
39. Porsolt RD, Bertin A, Blavet N, Deniel M, Jalfre M (1979) Immobility induced by forced swimming in rats: effects of agents which modify central catecholamine and serotonin activity. Eur J Pharmacol 57(2–3):201–210
40. Bortolato M, Godar SC, Davarian S, Chen K, Shih JC (2009) Behavioral disinhibition and reduced anxiety-like behaviors in monoamine oxidase B-deficient mice. Neuropsychopharmacology : official publication of the American College of Neuropsychopharmacology 34(13):2746–2757. doi:10.1038/npp.2009.118
41. Pellow S, Chopin P, File SE, Briley M (1985) Validation of open: closed arm entries in an elevated plus-maze as a measure of anxiety in the rat. J Neurosci Methods 14(3):149–167
42. Cui J, Zhang M, Zhang YQ, Xu ZH (2007) JNK pathway: diseases and therapeutic potential. Acta Pharmacol Sin 28(5):601–608. doi:10.1111/j.1745-7254.2007.00579.x
43. Anglade P, Vyas S, Javoy-Agid F, Herrero MT, Michel PP, Marquez J, Mouatt-Prigent A, Ruberg M et al (1997) Apoptosis and autophagy in nigral neurons of patients with Parkinson's disease. Histol Histopathol 12(1):25–31
44. Mizushima N, Hara T (2006) Intracellular quality control by autophagy: how does autophagy prevent neurodegeneration? Autophagy 2(4):302–304
45. Komatsu M, Kominami E, Tanaka K (2006) Autophagy and neurodegeneration. Autophagy 2(4):315–317
46. Li J, Li S, Zhang L, Ouyang L, Liu B (2015) Deconvoluting the complexity of autophagy and Parkinson's disease for potential therapeutic purpose. **Oncotarget**
47. Siracusa R, Paterniti I, Impellizzeri D, Cordaro M, Crupi R, Navarra M, Cuzzocrea S, Esposito E (2015) The association of palmitoylethanolamide with luteolin decreases neuroinflammation and stimulates autophagy in Parkinson's disease model. CNS Neurol Disord Drug Targets
48. Asakawa T, Fang H, Sugiyama K, Nozaki T, Hong Z, Yang Y, Hua F, Ding G et al (2016) Animal behavioral assessments in current research of Parkinson's disease. Neurosci Biobehav Rev 65:63–94. doi:10.1016/j.neubiorev.2016.03.016
49. Nakatogawa H, Suzuki K, Kamada Y, Ohsumi Y (2009) Dynamics and diversity in autophagy mechanisms: lessons from yeast. Nat Rev Mol Cell Biol 10(7):458–467. doi:10.1038/nrm2708
50. Spilman P, Podlutskaya N, Hart MJ, Debnath J, Gorostiza O, Bredesen D, Richardson A, Strong R et al (2010) Inhibition of mTOR by rapamycin abolishes cognitive deficits and reduces amyloid-beta levels in a mouse model of Alzheimer's disease. PLoS One 5(4):e9979. doi:10.1371/journal.pone.0009979
51. Hsieh CF, Lai YC, Pan RP, Pan CL (2008) Polarizing terahertz waves with nematic liquid crystals. Opt Lett 33(11):1174–1176
52. Simonsen A, Tooze SA (2009) Coordination of membrane events during autophagy by multiple class III PI3-kinase complexes. J Cell Biol 186(6):773–782. doi:10.1083/jcb.200907014
53. Kabeya Y, Mizushima N, Ueno T, Yamamoto A, Kirisako T, Noda T, Kominami E, Ohsumi Y et al (2000) LC3, a mammalian homologue of yeast Apg8p, is localized in autophagosome membranes after processing. EMBO J 19(21):5720–5728. doi:10.1093/emboj/19.21.5720
54. Mogi M, Nagatsu T (1999) Neurotrophins and cytokines in Parkinson's disease. Adv Neurol 80:135–139
55. Saha AR, Ninkina NN, Hanger DP, Anderton BH, Davies AM, Buchman VL (2000) Induction of neuronal death by alpha-synuclein. Eur J Neurosci 12(8):3073–3077
56. Levy OA, Malagelada C, Greene LA (2009) Cell death pathways in Parkinson's disease: proximal triggers, distal effectors, and final steps. Apoptosis 14(4):478–500. doi:10.1007/s10495-008-0309-3
57. McGeer PL, McGeer EG (2008) The alpha-synuclein burden hypothesis of Parkinson disease and its relationship to Alzheimer disease. Exp Neurol 212(2):235–238. doi:10.1016/j.expneurol.2008.04.008
58. Pal R, Tiwari PC, Nath R, Pant KK (2016) Role of neuroinflammation and latent transcription factors in pathogenesis of Parkinson's disease. Neurol Res 38(12):1111–1122. doi:10.1080/01616412.2016.1249997
59. Russo E, Andreozzi F, Iuliano R, Dattilo V, Procopio T, Fiume G, Mimmi S, Perrotti N et al (2014) Early molecular and behavioral response to lipopolysaccharide in the WAG/Rij rat model of absence epilepsy and depressive-like behavior, involves interplay between AMPK, AKT/mTOR pathways and neuroinflammatory cytokine release. Brain Behav Immun 42:157–168. doi:10.1016/j.bbi.2014.06.016
60. Saliba SW, Vieira EL, Santos RP, Candelario-Jalil E, Fiebich BL, Vieira LB, Teixeira AL, de Oliveira AC (2017) Neuroprotective effects of intrastriatal injection of rapamycin in a mouse model of excitotoxicity induced by quinolinic acid. J Neuroinflammation 14(1):25. doi:10.1186/s12974-017-0793-x
61. Citraro R, Leo A, Constanti A, Russo E, De Sarro G (2016) mTOR pathway inhibition as a new therapeutic strategy in epilepsy and epileptogenesis. Pharmacol Res 107:333–343. doi:10.1016/j.phrs.2016.03.039
62. Johnson GL, Lapadat R (2002) Mitogen-activated protein kinase pathways mediated by ERK, JNK, and p38 protein kinases. Science 298(5600):1911–1912. doi:10.1126/science.1072682
63. Gallo KA, Johnson GL (2002) Mixed-lineage kinase control of JNK and p38 MAPK pathways. Nat Rev Mol Cell Biol 3(9):663–672. doi:10.1038/nrm906